GPH-International Journal of Applied Science
(Online ISSN 3050-9653)
Volume 09 | Issue 10 | 2026
Published by: Global Publication House
DOI: https://doi.org/10.5281/zenodo.24274603
Available online at: www.gphjournal.org
Journal homepage: https://gphjournal.org/index.php/as/index

Influence of Viscous Damping on Harmonic-Oscillator Dynamics: Analytical Solutions, Numerical Verification, and Parameter-Recovery Uncertainty

MOHSIN HAMZAH ABED
Ministry of Education / Karbala Directorate of Education / Vocational Education Department
Corresponding e-mail: albwdymhsn664@gmail.com
&
HAYDER MOHSIN JASIM
College of Basic Education, Al-Mustansiriya University, Iraq
Corresponding e-mail: Haider_mohsen1993@uomustansiriyah.edu.iq

Abstract

An undamped harmonic oscillator forms an exact benchmark for studying dissipation, regime transitions and inverse parameter identification. In the present study, we offer a replicable analysis of the underdamped, critically damped, and overdamped cases of a linear mass-spring system with damping. Thanks to the analytical formulas for the displacement solutions, mechanical energy conservation, and the dimensionless damping ratio, as well as the use of the adaptive Runge-Kutta integrator, it becomes feasible to conduct a deterministic synthetic data-based estimation experiment that helps us to estimate the quality of the identification of the damping ratio based on the measured displacement time series. For the oscillator with mass 1 kg, stiffness of 100 N m^{-1}, and the initial displacement of 0.05 m, the natural frequency is equal to 10 rad/s, and the critical damping coefficient equals 20 N s/m. The analytical solution agrees with the numerical one up to the precision of the numerical method used, while the estimation experiment makes it possible to distinguish between the accuracy of modeling and errors in measurement. The study is offered as a computational benchmark without any claims on the new physics.

Keywords:

Damping; viscous damping; harmonic oscillator; logarithmic decrement; parameter estimation; energy dissipation; numerical verification; uncertainty quantification.

Highlights: Exact solutions for three dynamical regimes; mechanical energy balance; numerical cross-check; reproducible synthetic data estimation; limitations and laboratory validation proposed.

1. Introduction

Vibratory systems dissipate kinetic and elastic potential energy while vibratory forces convert mechanical energy to other forms. The most basic quantitatively tractable case assumes a linear spring and a velocity-dependent damping. While it describes a phenomenon described by an equation of utmost simplicity, it nevertheless retains its practical utility for the purposes of

© 2026 Author(s). Published by Global Publication House (GPH).
This is an Open Access article distributed under the terms of the CC BY 4.0 License.

instrumentation, vibration suppression, movement sensing, and numerical integration validation. The possibility of solving the problem analytically makes it an ideal framework for distinguishing between physical effects, solver effects, and parameter estimation uncertainty.

Damping affects both the transient amplitude decay envelope and the damped frequency of oscillations. It is not only a dampening of maximum amplitude but also a change in the pole structure of the system that ultimately results in stopping the oscillation process due to the critical level of damping and above. A key distinction that is often neglected is whether the damping coefficient c with units Ns/m and the damping ratio ζ without units are being referred to Earlier studies of damped vibrations have contributed to the development of the general theory of modal damping, including the conditions under which classical normal modes can exist [1,2]. Newmark introduced an essential computational model for the transient analysis of structure dynamics [3] and Dormand and Prince derived embedded Runge-Kutta formulas for controlled error integration [4]. Subsequent work by Little and Mann studied uncertainty in the estimate of the damping ratio by logarithmic decrement [5]. Such work inspires the examination of forward modeling against inverse inference as opposed to another demonstration of damped sinusoidal motion. The effect of damping on the frequency of linear systems was studied by Caughey and O'Kelly [6].

The classical model of viscous free-decay with three regimes of response is a known result rather than novel theoretical contribution [7]. In practice, though, nonlinearities and amplitude-dependent damping may render the assumption of constant viscous coefficient inadequate as is discussed in the literature on nonlinear system identification [8].

Vibration-based calibration of the models was already applied in the past [9]. Moreover, Hilbert transformation approaches were proposed for detecting amplitude dependence of the modes in free vibration immediately [10]. The mentioned sources serve as the inspiration for applying residual diagnostics and separation of inference and validation aspects.

1.1 Research questions

How does ζ affect the rate of decay, frequency, and shape of the transient response? (ii) How accurately can the precise viscous system be approximated using an adaptive numerical integrator? (iii) What information can be recovered on ζ from noisy displacement measurements, and how should uncertainties in this estimate be stated?

1.2 Scope and contribution

Contribution represents a coherent, well-documented case study, which includes an audit of energy savings as well as an inference procedure based on the Monte Carlo method. This model is typical; one can never say that there is something innovative just because of the presence of an analytic solution to a problem. It is mandatory for any future paper submitted to a journal to place itself in a methodological gap.

2. Mechanical model and assumptions

Consider a mass m attached to a spring with spring constant k, and a viscous damper of damping constant c. Displacements x are taken relative to the system equilibrium, hence the effect of gravity is removed. The body is taken as rigid, the spring, damper, and supporting structures

are considered massless, the damper acts with the force law Fd = -cẋ, and there is no time varying external forcing. All parameters are positive; only c = 0 is allowed for the limiting case of an undamped oscillator. [7]

$$m\,\ddot{x}(t) + c\,\dot{x}(t) + k\,x(t) = 0. \qquad (1)$$

Initial value problem needs $x(0)=x_0$ and $\dot{x}(0)=v_0$. All units used for the numerical illustration are listed in Table 1 below. There are no laboratory data presented in this paper.

Table 1. Physical parameters and computational assumptions.

Symbol	Meaning	Unit / selected value
m	oscillating mass	1.000 kg
k	linear stiffness	100.0 N m^{-1}
x_0	initial displacement	0.050 m
v_0	initial velocity	0.000 m s^{-1}
ω_n	natural angular frequency	10.000 rad s^{-1}
c	viscous coefficient	varies with ζ
ζ	damping ratio	0 to 2
σ	synthetic noise standard deviation	0.0004 m

2.1 Dimensional consistency

The restoring force kx is measured in N, the inertia term mẍ is measured in N, and the dissipation term cẋ is measured in N. Therefore, c is measured in kg/s or N·s/m. The mechanical energy at the beginning is $E_0 = kx_0^2/2 = 0.125$ J when $v_0=0$.

3. Nondimensional formulation and regimes

$$\omega_n = \sqrt{(k/m)}, \qquad ccr = 2\sqrt{(km)}, \qquad \zeta = c/ccr. \qquad (2)$$

Letting $\tau = \omega_n t$ and $X = x/x_0$ gives the dimensionalless form $X'' + 2\zeta X' + X = 0$, where primes represent differentiation with respect to τ. This approach lets us examine the influence of ζ independent of any units of measurement. [7]

$$X''(\tau) + 2\zeta\,X'(\tau) + X(\tau) = 0. \qquad (3)$$

If we have an exponential test $X \propto \exp(\lambda\tau)$, we get $\lambda^2 + 2\zeta\lambda + 1 = 0$. We obtain the two dimensionless poles $\lambda\pm = -\zeta \pm \sqrt{(\zeta^2-1)}$. The sign of the discriminant determines the type of reaction. If $0 < \zeta < 1$, there is a conjugated complex pole; if $\zeta=1$, there is a repeated root; if $\zeta > 1$, two different negative real roots are present. [6, 7]

$$\lambda\pm = -\zeta \pm \sqrt{(\zeta^2 - 1)}. \qquad (4)$$

3.1 Characteristic time scales

In case of underdamping, the decay time of the envelope will be $1/(\zeta\omega_n)$, while the angular frequency of the oscillation will be given by $\omega d = \omega_n \sqrt{(1 - \zeta^2)}$. In the vicinity of the critical damping, the oscillation period increases drastically, resulting in an erroneous conclusion about the non-oscillatory nature of the response for a short observation interval.

4. Closed-form solutions

4.1 Underdamped motion, $0 < \zeta < 1$

$$x(t) = e^{(-\zeta\omega_n t)} [\, x_0 \cos(\omega d t) + ((v_0+\zeta\omega_n x_0)/\omega d) \sin(\omega d t) \,]. \quad (5)$$

The sinusoidal term vibrates at ωd, while the exponential decay depends on the real component of the pole. As for the specified initial velocity of zero, the sine term must be such that $\dot{x}(0) = 0$, which is not satisfied by the expression $x_0 \exp(-\zeta\omega_n t)\cos(\omega d t)$. [7]

4.2 Critical motion, $\zeta = 1$

$$x(t) = [x_0 + (v_0+\omega_n x_0)t]e^{(-\omega_n t)}. \quad (6)$$

Repetition of the eigenvalue causes a linearly increasing factor. Although critical damping is the preferred method to achieve fast return without passing the equilibrium point, the fastest return depends on the particular criterion for performance and initial condition. [7]

4.3 Overdamped motion, $\zeta > 1$

$$x(t) = A \exp(r_1 t) + B \exp(r_2 t), \quad r_{1,2} = -\omega_n(\zeta \mp \sqrt{(\zeta^2 - 1)}). \quad (7)$$

$$A = (v_0 - r_2 x_0)/(r_1 - r_2), \qquad B = x_0 - A. \quad (8)$$

While higher damping reduces oscillations, very high ζ causes the pole r_1 to become very slowly decaying $r_1 \approx -\omega_n/(2\zeta)$. Overdamping is thus not the same as very rapid settling. The exact formulas give a standard to compare to numerical results without comparing only graphs that could be deceptive. [7]

5. Energy dissipation and physical consistency

$$E(t) = \tfrac{1}{2}m[\dot{x}(t)]^2 + \tfrac{1}{2}k[x(t)]^2. \quad (9)$$

By multiplying Equation (1) by the velocity and rearranging the terms, we obtain an exact expression for the energy balance, which illustrates how viscous damping dissipates mechanical energy from the system:

$$dE/dt = -c[\dot{x}(t)]^2 \leq 0. \quad (10)$$

$$E(t) + \int_0^t c[\dot{x}(s)]^2 \, ds = E(0). \quad (11)$$

This equation is much more basic than any other related to decrease in amplitude since it holds at all times in a real solution. Energy never rises, not even while exchanging from kinetic and elastic energies. In case c = 0, then energy remains constant, and in case c > 0, then energy drops except at certain points where velocity equals zero.

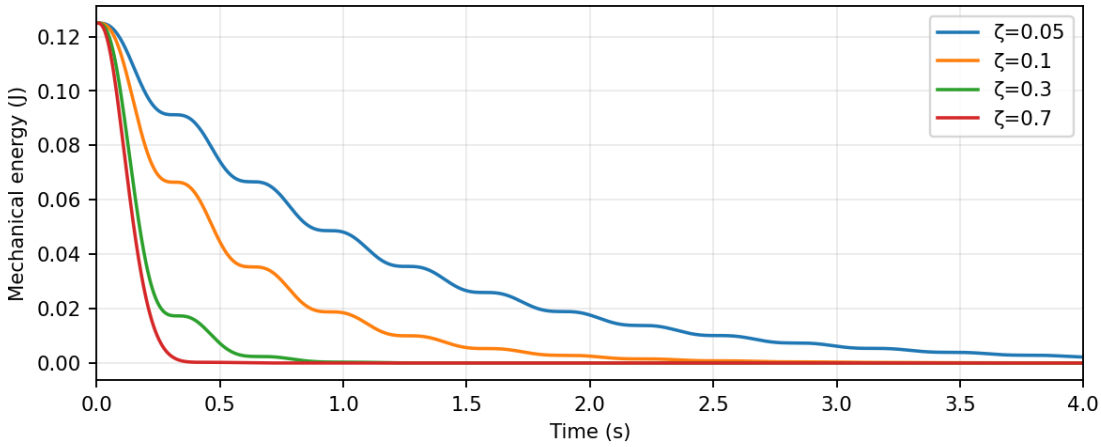

Figure 1. Computed total mechanical energy for four underdamped ratios.

The numerical approach can evaluate Eq. (11) by using trapezoidal quadrature of c v^2 with respect to E(0), and so this discrepancy represents quadrature error rather than the breaking of any physical conservation law.

6. Computational methodology

The first-order state vector y=(x,v) follows $\dot{y}=(v, -(c/m)v-(k/m)x)$. All forward solutions were calculated on a grid consisting of 2401 equally spaced points in the range of $0 \leq t \leq 8$ s. The numerical integration was done continuously using fifth order Runge-Kutta method with error estimation (RK45) and tolerance of 10^{-10} and 10^{-12} respectively. The analytical solution was obtained independently using an appropriate formula of the damping regime. [11]

$$dy/dt = [v, -2\zeta\omega_n v - \omega_n^2 x]^T. \quad (12)$$

The computational process was comprised of the following steps: parameter definition in SI units; evaluation of ω_n and ccr; selection of values of ζ; calculation of state equations; analysis of response curves; computation of displacements errors; calculation of kinetic and elastic energy and figure plotting with properly labeled axes and units. Numerical array processing and error-controlled integration were carried out using methods consistent with the NumPy and SciPy scientific-computing libraries [12, 13]. A fixed pseudorandom seed of 2026 was employed to generate synthetic noise, ensuring that the parameter-identification trials could be repeated and their results reproduced consistently.

6.1 Accuracy metric

$$\varepsilon\infty = max_t\ |xRK45(t) - xexact(t)|. \quad (13)$$

Nonetheless, this is not backed up experimentally as it is only possible to numerically validate the correctness of the theoretical equations, but not to prove the exact viscous damping of a particular oscillator. This is clearly indicated in both the Results and Discussion sections of this study. [11]

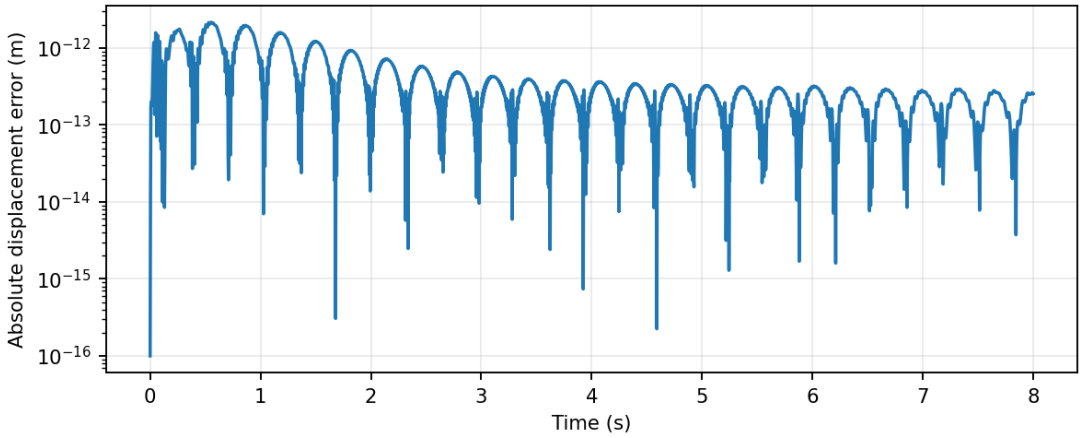

Figure 2. Absolute displacement error of high-tolerance RK45 and the exact solution for ζ=0.20.

7. Forward-model results: displacement

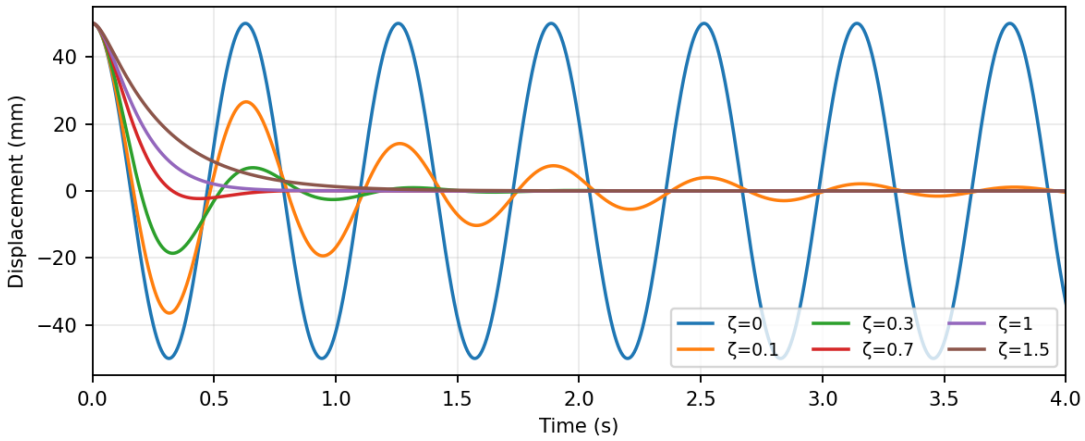

Figure 3. Displacement histories for six values of damping ratio, with fixed mass, stiffness and initial conditions.

The change in trajectory due to damping in a quantitative sense is depicted in Fig. 3. For ζ=0, the oscillations are periodic and do not tend to zero. For ζ=0.10 and 0.30, there are oscillations crossing the equilibrium state with decreasing envelope. For ζ=0.70, the transient state becomes significantly smaller, while the damped period becomes larger. For the critical damping case of ζ=1, there are no oscillations, while ζ=1.5 includes both fast and slow exponential terms.

In this parametrization, the physical damping coefficient is $c=20\zeta$ N s m^{-1}. Therefore, the cases shown above include the values of the coefficient c equal to 0, 2, 6, 14, 20 and 30 N s m^{-1}. With the constant stiffness k and mass m, the variation of the damping coefficient c changes the decay constant and oscillation frequency for ζ

8. Forward-model results: phase geometry

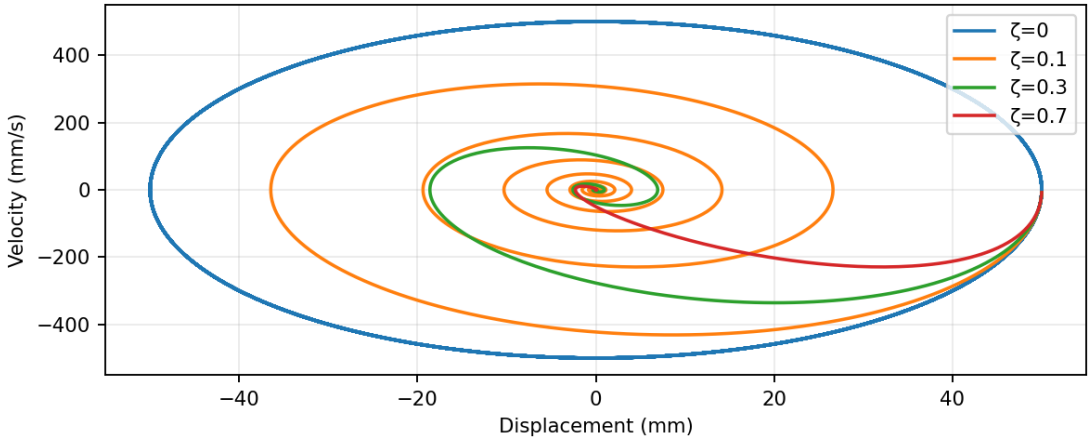

Figure 4. Velocity–displacement trajectories for four damping ratios; the undamped orbit is closed.

The phase trajectories present another method to characterize the transient behavior. Without dissipative effects, the trajectory will be a closed curve that will trace an ellipse in the (x,v) space, as it represents the conservation of mechanical energy. With viscous friction, there will be trajectories that are spirals into the origin in the underdamped region. As the value of ζ increases, the spiral becomes tighter and the number of rotations decreases. [7]

8.1 Damped frequency

$$\omega d/\omega_n = \sqrt{(1-\zeta^2)},\ for\ 0 \le \zeta < 1. \qquad (14)$$

Equation (14) is a spectral signature of damping based on the model assumptions made. This gives a decreasing oscillation frequency as ζ increases, with no oscillation frequency at critical damping. A spectral estimation of the decayed signal is subject to bias due to the use of windowing and noise; hence it is better to fit the complete time-domain signal to avoid any assumption of unbiasedness of the ωd. [14]

9. Identification of damping from time records

The spectral signature of damping is given by Equation (14). This equation predicts that the oscillatory frequency will decrease as a function of ζ and loss of real oscillatory frequency due to critical damping. The estimation of the spectral frequency from a decaying record may be biased due to the effects of windowing and noise, but fitting the complete time-domain data circumvents the need for the Fourier transform assumption of unbiasedness of ωd. [14]

$$\delta = ln(Aj/Aj+1) = 2\pi\zeta/\sqrt{(1-\zeta^2)}. \qquad (15)$$

$$\zeta = \delta/\sqrt{(4\pi^2+\delta^2)}. \qquad (16)$$

The second estimator employed for the second time uses observation intervals ti = 0.01i s, where i = 0,..., 499. Artificial displacements are generated through adding to the exact displacement independently normally distributed zero mean noise of standard deviation σ = 0.0004 m on the exact response at ζtrue = 0.18. The only unknown estimated is ζ, where m, k,

x_0, and v_0 are known. Constrained nonlinear least-squares minimizes the normalized squared residual on $0.001 \leq \zeta \leq 0.99$.

[15, 16].

$$\zeta = \text{argmin}_\zeta \Sigma_i [(y_i - x(t_i;\zeta))/\sigma]^2. \quad (17)$$

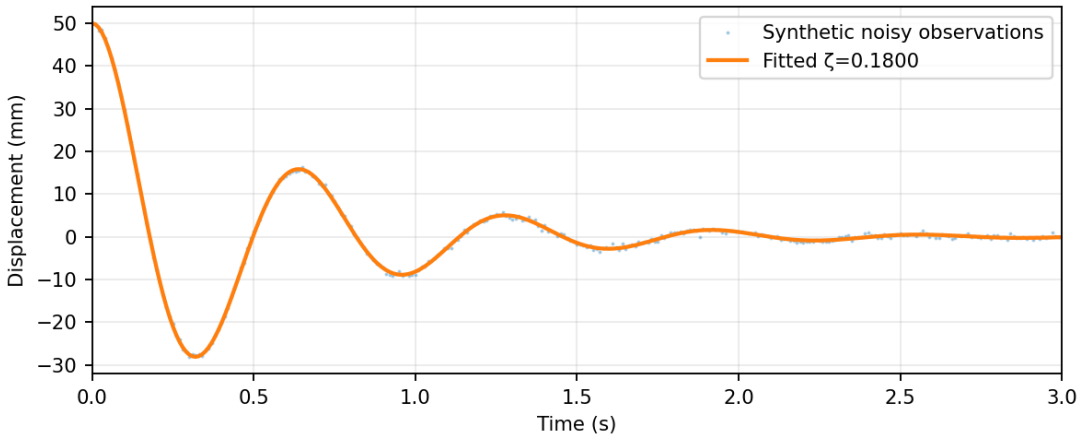

Figure 5. A single noise-contaminated synthetic displacement record and the fitted viscous-damping model.

10. Repeated-trial uncertainty analysis

In order to estimate sampling variability rather than depend on a single lucky realization of the noise, 250 independent realizations were created based on the same physical parameter, sampling mesh and Gaussian noise. All of them were estimated independently using the exact forward response and the same bounds. Simulated estimates create the Monte-Carlo distribution under the assumption of the specific data model. According to known standards related to estimation of uncertainty and distribution propagation, such a simulation represents the uncertainty given specific inputs [17, 18]. The sample standard deviation gives the variability of the estimator, and it is not meant to be the uncertainty limit for model discrepancy.

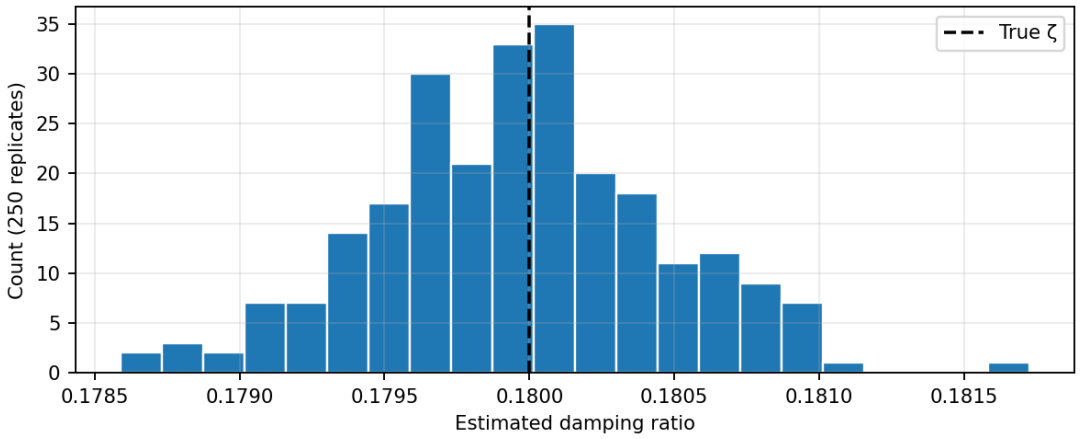

Figure 6. Distribution of 250 fitted damping ratios from independent synthetic records; dashed line is ζtrue=0.18.

Table 2. Monte Carlo outcome; numerical values depend on the declared random seed and are simulation results, not measured material properties.

Quantity	Computed value
Number of synthetic repeats	250
True damping ratio	0.180000
Mean of fitted ratios	0.179959
Standard deviation	0.000499
Empirical 2.5% / 97.5% quantiles	0.178994 / 0.180953
First illustrated fit	0.180004

11. Discussion and robustness

Evidence is presented in three forms: analytical verification of the linearity of the model, numerical validation of agreement with the known solution, and statistical performance from simulations. These serve different purposes. Analytical expressions provide the relation between ζ and poles of the oscillator; numerical discrepancies test the differential-equation solver; and Monte Carlo simulation provides consistency under the conditions set by the choice of observational and noise models. No evidence can verify that all physical dashpots are linear and their model parameters do not change while moving. [11]

The practical difficulty is the question of structural identifiability with several unknown parameters. Given only the free-decay displacement response, the model predicts the combinations $\omega_n=\sqrt{(k/m)}$ and $\zeta=c/(2\sqrt{(km)})$. With no independent information on the mass, the values of all three m, c and k cannot be individually determined. It would thus be an exaggeration to treat the individual parameters as being independently identifiable from one free-decay experiment. [16]

Other sources of difference could be dry friction, amplitude-dependence of losses, compliance of the support, sensor drifts, imperfections of releasing from rest, nonlinearity of the spring, and frequency-dependent dissipation. The tell-tale signs of these would be structured residuals, a non-exponential decay, and changes of parameter estimates with the choice of fit intervals. An extension worth pursuing would be a comparison of different types of models using withheld validation data and model selection. [8–10]

11.1 Model limitations

For the Monte Carlo simulation, independent Gaussian noise of known variance and true parameters are assumed. Correlated sensor noise, finite resolution, and any calibration errors have not been taken into consideration. The number of samples selected is sufficient to provide a representative sampling distribution for illustrative purposes but not enough for any conclusions to be made on tail probabilities. There is also another well-known method for the estimation of sampling uncertainty through bootstrap resampling [19], which has not been used in this current Monte Carlo simulation study.

12. Proposed laboratory validation

The computational benchmark may be used for an experimental paper by fixing a low-friction horizontal cart or vertical mass spring system fitted with an optical sensor and a controllable viscous damper. Weigh the mass using a weighing scale while determining the value of k in

static tests. Displace the mass by about 50 mm, release it without any impulse at frequencies of ≥200 Hz and record ten or more nominal oscillations where possible, depending on the decay time. [7, 14]

Do this at least five times independently for each fixed value of the damper. Estimate c from nonlinear regression of Eq. (5) without assuming known initial conditions if their imprecision is significant. Designate in advance diagnostics of the model: residual autocorrelation, trial-to-trial reliability, dependence on fitting window width, and the agreement between time-domain and logarithmic-decrement estimates. Time calibration and measurement precision, instrument resolution, and error propagation from m and k into ζ should be included in the analysis. [5, 15-18]

12.1 Acceptance criteria and reproducibility

A laboratory claim should provide measurements of displacement traces, calibration documentation of instruments, availability of raw data, list of excluded samples, residual plots, and uncertainties of the nonlinear fit. The computational part is reproducible by running Eq. (12) with the parameters from Table 1 and Eqs. (15)-(17) for the experiment design. A journal-ready archive should include executable code, versioned software dependencies, raw data file, and README, consistent with the FAIR principles of data stewardship [20]. In the absence of the archive, the manuscript would be considered analytical/computational research rather than an experiment.

12.2 Research ethics and transparency

No observations with instrumental sensors were fabricated. Synthetic observations are applied in the inverse problem without any ambiguity. Issues of conflict of interests, funding, authorship, availability of data, and any other disclosures necessary for the target journal need to be completed by the relevant researcher before submission. Any text generation assistance must be disclosed in case it is needed by the target journal; the authors take full responsibility for all statements and references in the paper.

13. Conclusions

Damping in the viscous regime controls the transient behavior of the harmonic oscillator using the nondimensional damping ratio ζ. Analytical solutions provide conditions for underdamping, critical damping, and overdamping and the energy dissipation formula $dE/dt=-cv^2$ for the conservative energy E of the idealized oscillator. Adaptive high-accuracy integration generates the analytical solution as a check of the computational method. A fully developed case study with synthetic noise illustrates the identification of the damping parameters and the dependence of the quantification of uncertainty on the model assumptions for the measurement. This paper offers the reproducible computational and mathematical baseline; physical generality and novelty needed for publication demand independent measurements.

References

1. Caughey, T. K. (1960). Classical normal modes in damped linear dynamic systems. Journal of Applied Mechanics, 27(2), 269–271. https://doi.org/10.1115/1.3643949
2. Caughey, T. K., & O'Kelly, M. E. J. (1965). Classical normal modes in damped linear dynamic systems. Journal of Applied Mechanics, 32(3), 583–588. https://doi.org/10.1115/1.3627262
3. Newmark, N. M. (1959). A method of computation for structural dynamics. Journal of the Engineering Mechanics Division, 85(3), 67–94. https://doi.org/10.1061/JMCEA3.0000098
4. Dormand, J. R., & Prince, P. J. (1980). A family of embedded Runge–Kutta formulae. Journal of Computational and Applied Mathematics, 6(1), 19–26. https://doi.org/10.1016/0771-050X(80)90013-3
5. Little, J. A., & Mann, B. P. (2019). Optimizing logarithmic decrement damping estimation through uncertainty propagation. Journal of Sound and Vibration, 457, 368–376. https://doi.org/10.1016/j.jsv.2019.05.040
6. Caughey, T. K., & O'Kelly, M. E. (1961). Effect of damping on the natural frequencies of linear dynamic systems. Journal of the Acoustical Society of America, 33(11), 1458–1461. https://doi.org/10.1121/1.1908470
7. Den Hartog, J. P. (1956). Mechanical Vibrations (4th ed.). McGraw-Hill.
8. Kerschen, G., Worden, K., Vakakis, A. F., & Golinval, J.-C. (2006). Past, present and future of nonlinear system identification in structural dynamics. Mechanical Systems and Signal Processing, 20(3), 505–592. https://doi.org/10.1016/j.ymssp.2005.04.008
9. Mottershead, J. E., & Friswell, M. I. (1993). Model updating in structural dynamics: A survey. Journal of Sound and Vibration, 167(2), 347–375. https://doi.org/10.1006/jsvi.1993.1340
10. Feldman, M. (1994). Non-linear system vibration analysis using Hilbert transform—I. Free vibration analysis method "FREEVIB". Mechanical Systems and Signal Processing, 8(2), 119–127. https://doi.org/10.1006/mssp.1994.1011
11. Oberkampf, W. L., & Trucano, T. G. (2002). Verification and validation in computational fluid dynamics. Progress in Aerospace Sciences, 38(3), 209–272. https://doi.org/10.1016/S0376-0421(02)00005-2
12. Virtanen, P., Gommers, R., Oliphant, T. E., et al. (2020). SciPy 1.0: Fundamental algorithms for scientific computing in Python. Nature Methods, 17, 261–272. https://doi.org/10.1038/s41592-019-0686-2
13. Harris, C. R., Millman, K. J., van der Walt, S. J., et al. (2020). Array programming with NumPy. Nature, 585, 357–362. https://doi.org/10.1038/s41586-020-2649-2
14. Bendat, J. S., & Piersol, A. G. (2010). Random Data: Analysis and Measurement Procedures (4th ed.). Wiley. https://doi.org/10.1002/9781118032428
15. Marquardt, D. W. (1963). An algorithm for least-squares estimation of nonlinear parameters. Journal of the Society for Industrial and Applied Mathematics, 11(2), 431–441. https://doi.org/10.1137/0111030
16. Ljung, L. (1999). System Identification: Theory for the User (2nd ed.). Prentice Hall PTR. ISBN 978-0-13-656695-3
17. JCGM. (2008). Evaluation of measurement data—Guide to the expression of uncertainty in measurement (JCGM 100:2008). Joint Committee for Guides in Metrology. https://doi.org/10.59161/JCGM100-2008E

18. JCGM. (2008). Evaluation of measurement data—Supplement 1: Propagation of distributions using a Monte Carlo method (JCGM 101:2008). Joint Committee for Guides in Metrology. https://doi.org/10.59161/JCGM101-2008
19. Efron, B. (1979). Bootstrap methods: Another look at the jackknife. The Annals of Statistics, 7(1), 1–26. https://doi.org/10.1214/aos/1176344552
20. Wilkinson, M. D., Dumontier, M., Aalbersberg, I. J. J., et al. (2016). The FAIR Guiding Principles for scientific data management and stewardship. Scientific Data, 3, 160018. https://doi.org/10.1038/sdata.2016.18